Research Square

Preprints are preliminary reports that have not undergone peer review.
They should not be considered conclusive, used to inform clinical practice,
or referenced by the media as validated information.

Adaptive Neural Network Control for Sensorless DC Motor Speed Regulation in Electric Vehicles under Road Disturbances

Nitendra kumar

nitendra21_rs@ei.nits.ac.in

National Institute Of Technology Silchar

Vipin Chandra Pal

National Institute Of Technology Silchar

Akshaya kumar Pati

Kalinga Institute of Industrial Technology

Sheetla Prasad

Galgotias University

Research Article

Keywords: Sensorless control, Neural network, Adaptive control, Electric vehicle, DC motor, Road disturbance, Lyapunov stability

Posted Date: November 13th, 2026

DOI: https://doi.org/10.21203/rs.3.rs-11354505/v1

License: This work is licensed under a Creative Commons Attribution 4.0 International License.
Read Full License

Additional Declarations: No competing interests reported.

Adaptive Neural Network Control for Sensorless DC Motor Speed Regulation in Electric Vehicles under Road Disturbances

Abstract

Regulating the speed of an electric vehicle (EV) drive is hard: the dynamics are nonlinear, the motor parameters are never known exactly, and the road keeps changing the load. This paper presents a disturbance-aware adaptive sensorless neural network controller (DAAS-NNC) for a DC motor drive in an EV. A neural network estimates the disturbance online, and an adaptive learning law driven by the error derivative tunes the controller, improving the transient response and robustness without affecting steady-state accuracy. The controller needs no mechanical speed sensor, which lowers hardware cost and removes a component that can fail. A Lyapunov-based adaptive law keeps the closed-loop system stable and all signals bounded. The controller is tested for speed tracking, load variation, and sloped and banked road profiles. In simulation, DAAS-NNC reduces the rise time by 44.4% and 21.9% and the settling time by 55.6% and 33.3% relative to conventional PI and MRAS controllers, respectively, and cuts the overshoot from 12.3% (PI) and 5.6% (MRAS) to 1.8%. It also reduces speed deviations, produces smoother control inputs with fewer oscillations, and lets the neural network estimator converge quickly. These results point to DAAS-NNC as a promising controller for EV powertrains.

Keywords: Sensorless control, Neural network, Adaptive control, Electric vehicle, DC motor, Road disturbance, Lyapunov stability

1 Introduction

The accelerated development of electric vehicles (EV) has increased the pressure on high-performance, efficient, and reliable motor control methods that can work under nonlinear dynamics, parameter uncertainties, and external disturbance. Accurate speed control, along with the high level of robustness and control action, is a major challenge of modern EV drive systems. Traditional controllers like proportional integral (PI) and model reference adaptive system (MRAS)-based systems, as commonly used, tend to be less flexible and poorer in performance when used in different operating conditions. Recent progress in intelligent control has emphasized the usefulness

of neural network-based methods to deal with nonlinearities and uncertainties. Specifically, the physics-informed neural networks (PINNs) have gained significant concern because they can enforce physical laws into the learning process, which enhance the model fidelity, data efficiency and robustness [1]. Nevertheless, in spite of these benefits, the computational intensive nature of PINN-based methods, and the fact that they are mostly investigated in fault diagnostics and modeling, as opposed to real-time control execution in EV drives. The sensorless control methods have also acquired great importance because of their capability to lower the cost of the system, improve the reliability and avoid the reliance on the mechanical sensors. Improved performance has been shown with various approaches, such as MRAS-based estimation and model predictive control (MPC) in electric drive applications [2]-[3]. Also, sensorless cost-effective methods based on minimized sensor setups have been designed to be practically implemented in motor drives [4]. However, they tend to be based on correct system models and can be characterized by poor performance to rapidly changing disturbances. Adaptive and observer-based control strategies have been suggested to increase robustness. Perturbation observers have demonstrated greater disturbance rejection and tracking accuracy with nonlinear adaptive controllers [5] . More sophisticated methods of estimation in motor drives use hybrid estimation methods that are a combination of machine learning and estimates that are obtained through the use of observers like extended Kalman filters [6] . Additionally, the compensation schemes based on neural networks and combined with advanced control strategies, including sliding-mode, and backstepping approaches, have been shown to be more dynamic over uncertainties [7] . Recent advances in neuro-fuzzy and intelligent observer based systems also suggest an improvement of accuracy of estimation and a decrease of ripple effects within the motor control systems [8] . Despite these advancements, existing approaches exhibit several limitations. The majority of sensorless and intelligent control approaches fail to explicitly combine the disturbance-aware estimation with the adaptive learning processes within a common framework. Moreover, most approaches either require proper modeling of the system or do not guarantee a smooth control action in the presence of robustness with respect to the rapidly changing and nonlinear disturbances. Such constraints limit their use in real-time EV drive systems, where performance and computational efficiency are paramount. In order to overcome these difficulties, this paper introduces a Disturbance-Aware Adaptive Sensorless Neural Network Controller (DAAS-NNC) to high-performance motor control. The suggested framework combines neural network-based disturbance estimation with an error-derivative adaptive learning mechanism, which allows to improve transient response and enhance disturbance rejection without deteriorating steady-state performance. Moreover, the sensorless design enhances feasibility in practice, by removing the requirement of mechanical speed sensors.

1.1 The main contributions of this work are summarized as follows

- Proposes a disturbance-aware adaptive neural network controller for sensorless motor drive systems.

- Introduces an error derivative learning mechanism to enhance transient dynamics without affecting steady-state behavior.
- Develops a Lyapunov-based adaptive learning law ensuring boundedness and closed-loop stability.
- Demonstrates superior performance in terms of tracking accuracy, disturbance rejection, and control smoothness under realistic operating conditions.

The suggested framework offers a computationally effective and practically feasible solution to next-generation intelligent EV drive systems.

This paper is structured as follows. Section 2 presents the related work and research gaps. Section 3 describes the proposed DAAS-NNC methodology. Section 4 covers simulation results and performance evaluation. Finally, Section 6 concludes the paper.

2 Literature Review

2.1 Intelligent and Hybrid Sensorless Control Techniques

The recent literature has examined hybrid intelligent methods to improve the sensorless motor control performance [9] In this suggested a PSO-trained ANFIS-based ANFIS controller of PMBLDC motors that enhances the accuracy of estimations by using hybrid learning and zero-crossing detection. In a similar manner[10] combined ANFIS and MRAS to improve both robustness and dynamic behavior when the parameter uncertainties and the load are uncertain. In a different method, [11] applied an RBFNN-based hybrid optimization to the BLDC motor speed control, and it obtained a better transient response and a less steady-state error. The methods enhance adaptability and performance but they usually have complicated hybrid structures, which can raise the computational load and restrict real-time applicability.

2.2 Neural Network-Based Estimation Methods

Estimation methods based on neural networks have been studied extensively to be used in sensorless control. [12] formed ANN-based position and speed estimation of BLDC motors, with high position estimation accuracy, and marginally improved speed estimation compared to traditional techniques. Also, [13] have shown that neural network adaptive controllers are capable of effectively enhancing speed control in generator systems.

2.3 Observer-Based and Sliding-Mode Control Approaches

The observer-based techniques still shine through their resilience to uncertainties. This introduced a super-twisting sliding mode observer with a fractional order, having lower steady-state error and higher robustness levels [14]. On the same note, [15] proposed a fuzzy sliding-mode observer that minimizes chattering and improves estimation capabilities.

2.4 Adaptive and Robust Control Strategies

Adaptive control methods have been designed to deal with system uncertainties and disturbances [16]. Developed an adaptive sliding-mode control law of sensorless induction motors, which proved to be resistant to changes in parameters and external interferences.

2.5 Model-Based and Predictive Control Methods

Electric drive systems have extensively used model-based and predictive control strategies. It was studied the control of EV traction systems with DTC-SVM, with less torque ripple and better speed regulation [17]. Likewise, [18] introduced a feedforward-loop phase-locked loop control of sensorless IPMSM drives, which enhances accuracy of the estimation of the state during harmonic perturbations.

2.6 Emerging Intelligent and Data-Driven Approaches

The recent studies have broadened to intelligent and data-driven approaches in addition to the conventional motor control [19]. have suggested a hybrid physics-informed observer-based architecture to sensorless estimation and have shown that it is more robust to nonlinear systems. A data-driven optimization-based framework of energy management in EV applications, which is based on reinforcement learning was proposed [20] . Moreover, [21] underscored the importance of artificial intelligence and predictive control in enhancing the performance of EV power electronics.

2.7 Optimized Control Strategies for EV Drive

Control methods that utilize optimization have also been considered in order to improve motor performance. A modified field oriented field-based control strategy proposed by [22] demonstrated with optimization based tuning demonstrates a lower torque ripple and a better performance in the EV application.

2.8 Research Gap

From the above studies, several limitations can be identified: Existing approaches focus primarily on estimation accuracy or control performance independently, without integrating both in a unified framework.
Neural and hybrid approaches enhance flexibility and can be complex to compute, hindering real-time use.
Observer-based and sliding-mode methods are not only robust, but also have tuning complexity problems and chattering.
Model-based and predictive approaches require precise system models, and are less effective with nonlinear disturbances. Notably, the existing literature does not present an explicit control framework that combines disturbance-adaptive estimation and adaptive learning using error dynamics in a sensorless setup.

3 Methodology

3.1 Electric Vehicle Drive System

The electric vehicle (EV) drive system comprises of DC power source, PWM based converter, DC motor and sensorless adaptive control unit as ashown in Figure 1. The controller controls the motor speed due to different loads situations, such as road profile disturbances. The dynamic behavior of the DC motor is described by coupled electrical and mechanical equations.

Electrical Dynamics

$$V_a(t) = R_a i_a(t) + L_a \frac{di_a(t)}{dt} + K_e \omega(t) \tag{1}$$

Mechanical Dynamics

$$J \frac{d\omega(t)}{dt} = K_t i_a(t) - B\omega(t) - T_L(t) \tag{2}$$

Eq. (1) and Eq. (2) is the electromechanical interaction in which the armature current produces torque and the rotor speed causes the back electromotive force.

Reduced Speed Dynamics

To design its control, the system is put in a reduced form by adding the electrical dynamics to the mechanical equation:

$$\dot{\omega}(t) = -a\omega(t) + bV_a(t) - d(t) \tag{3}$$

where:

$$a = \frac{B}{J} + \frac{K_t K_e}{JR_a}, b = \frac{K_t}{JR_a}, d(t) = \frac{1}{J} T_L(t)$$

Problem Formulation

Let $\omega_r(t)$)denote the reference speed. The error of tracking is:

$$e(t) = \omega_r(t) - \omega(t) \tag{4}$$

The control objective is to design the input voltage $V_a(t)$ such that the tracking error remains bounded:

$$|e(t)| \leq \delta \tag{5}$$

in the presence of unknown disturbance $T_L(t)$and system uncertainties.

3.2 Sensorless Speed Estimation

In practical EV drive systems, the use of mechanical speed sensors increases cost and reduces reliability. Thus, only electrical quantities that are measurable, such as armature voltage and current, are used to estimate the rotor speed.

Based on the electrical dynamics of Eq. (1), the rotor speed can be determined as:

$$\omega(t) = \frac{1}{K_e} \left(V_a(t) - R_a i_a(t) - L_a \frac{di_a(t)}{dt} \right) \tag{6}$$

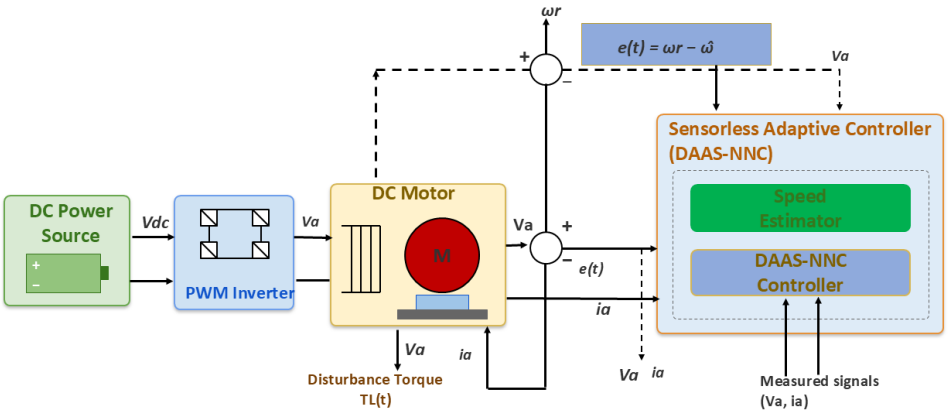


Fig. 1 EV Drive System Architecture

The direct algebraic estimation of speed is given in Eq. (6) . The term $\frac{di_a(t)}{dt}$is however, is very sensitive to measurement-noise, which can reduce the accuracy of the estimation in real-time implementation.

To reduce this problem, an estimator based on neural networks is proposed to estimate the nonlinear mapping between electrical variables and rotor speed. The approximate speed is determined as:

$$\widehat{\omega}(t) = \mathcal{N}_\theta \left(V_a(t), i_a(t), \dot{i}_a(t) \right) \tag{7}$$

where:

- $\mathcal{N}_\theta(\cdot)$denotes a parametric neural network with weight vector θ,
- $\widetilde{\dot{i}}_a(t)$is a filtered version of the current derivative to reduce noise effects.

The neural estimator uses the universal approximation property of feedforward networks to model the nonlinear term in Eq. (6) without actually calculating the derivative term.

Estimation Error Definition

The estimation error is defined as:

$$\widetilde{\omega}(t) = \omega(t) - \widehat{\omega}(t) \tag{8}$$

Assumption A1 (Bounded Estimation Error)

We assume that the neural estimator has limited approximation error:

$$|\widetilde{\omega}(t)| \leq \varepsilon_\omega \tag{9}$$

where $\varepsilon_\omega > 0$ is a small constant dependent on network approximation capability and filtering accuracy.

Justification of Assumption A1

The fact that the estimation error is bounded is based on two practical considerations:

1. **Universal Approximation Property**

   Feed forward neural networks are able to model any non-linear continuous function over a small range with an arbitrary degree of accuracy. As the mapping in Eq. (6) is a continuous one with respect to $V_a$and i_a, there exists an optimal parameter vector θ^*such that:

$$\omega(t) = \mathcal{N}_{\theta^*}(x) + \varepsilon(t) \tag{10}$$

where $x = [V_a, i_a, \widetilde{i}_a]$and $\mid \varepsilon(t) \mid \leq \varepsilon_\omega$.

2. **Bounded Input Signals**

   The system states and inputs are bounded, as per Section 3.1. Thus, the neural network will be working on a small input space, which guarantees a limited approximation error.

From Eq. (8) Eq. (10) , it follows that:

$$|\widetilde{\omega}(t)| \leq \varepsilon_\omega \tag{11}$$

which establishes that the estimation error is uniformly bounded.

3.3 Disturbance Modeling under Road Conditions

When operating electric vehicles in practice, the load torque on the DC motor is highly dependent on external driving conditions including road slope and banking. These effects add extra torque load, which directly affects the motor speed and the performance of the system as shown in Figure 2.

The total load torque is expressed as:

$$T_L(t) = T_{roll} + T_{aero} + T_{grade}(t) + T_{bank}(t) \tag{12}$$

where $T_{roll}$and T_{aero}represent the nominal components associated with rolling resistance and aerodynamic drag, while $T_{grade}(t)$and $T_{bank}(t)$account for variations due to road conditions.

The effect of road slope is modeled as:

$$T_{grade}(t) = r\, mg \sin(\theta(t)) \tag{13}$$

where $\theta(t)$ represents the angle of inclination of the road. This element adds the amount of torque needed when climbing a hill and subtracts it when descending.

Similarly, the influence of road banking is represented as:

$$T_{bank}(t) = r\, mg\kappa_b \sin(\phi(t)) \tag{14}$$

where $\phi(t)$is the bank angle and $\kappa_b$is a scaling factor representing its effective contribution to longitudinal dynamics.

For control design, the load torque in Eq. (12) is expressed in a simplified form as:

$$T_L(t) = \bar{T} + \Delta(t) \tag{15}$$

where $\bar{T}$denotes the nominal load component and $\Delta(t)$represents the combined effect of slope and banking disturbances.

To design the control, the load torque in Eq. (12) can be simplified as:

$$T_L(t) = \bar{T} + \Delta(t) \tag{16}$$

where $\bar{T}$represents the nominal component (rolling and aerodynamic effects), and $\Delta(t)$denotes the variation due to road conditions such as slope and banking.

The disturbance term is assumed to be bounded:

$$|\Delta(t)| \leq \Delta_{\max} \tag{17}$$

The banking element is formulated as a near longitudinal disturbance to be used in control formulations. Despite the fact that banking has a major impact on the lateral vehicle behavior, its effect on the traction demand is represented by the lumped disturbance term T_bank (t), allowing a simplified, but effective, representation to be used in control design. Its representation Eq. (15) can be used to consider the EV drive system as a system with an unknown but bounded disturbance input, which can be counteracted through adaptive control methods. The formulation is the direct support of the creation of the suggested sensorless neural network controller in the next section.

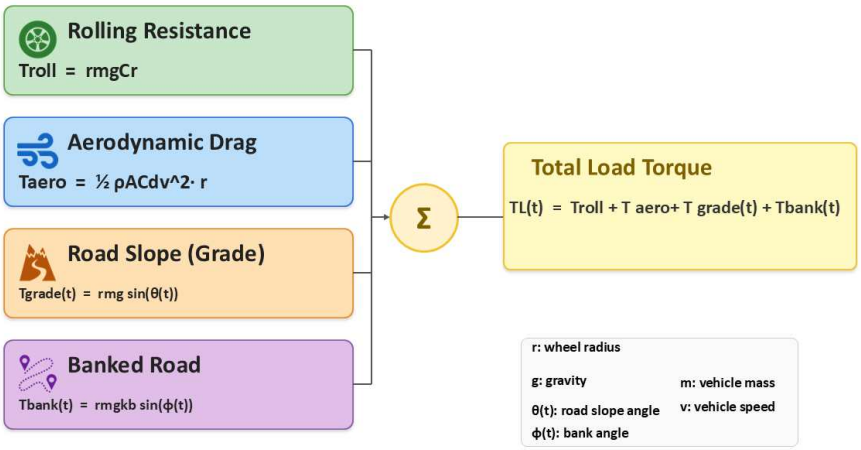


Fig. 2 Road Disturbance Representation

3.4 Reduced Dynamic Model

Using the motor dynamics in Eq. (2)and the disturbance representation in Eq. (16) , the speed dynamics of the EV drive system can be formulated in a concise form that can be used in the design of controllers.

Substituting the load torque into the mechanical equation yields:

$$\dot{\omega}(t) = -a\,\omega(t) + b\,i_a(t) - d(t) \tag{18}$$

where:

$$a = \frac{B}{J}, b = \frac{K_t}{J}, d(t) = \frac{1}{J}T_L(t)$$

The electrical dynamics are added in order to provide a relationship between the control input and the system, resulting in:

$$\dot{\omega}(t) = -a\,\omega(t) + b\,V_a(t) - d(t) \tag{19}$$

where $V_a(t)$is the control voltage applied through the PWM converter.

As we shall see in Eq. (19) , the EV drive system can be modeled as a first-order system with an additive disturbance term. The disturbance $d(t)$ sums up all the external effects due to road conditions and uncertainties.

The structure is especially appropriate to adaptive control design, where the disturbance may be estimated and compensated without explicit measurement.

3.5 Proposed DAAS-NNC Controller

A Disturbance-Aware Adaptive Sensorless Neural Network Controller (DAAS-NNC) is proposed to regulate the motor speed under uncertain operating conditions.

The proposed method compares with the traditional MRAS-based methods that are based on linear adaptation mechanisms, but it uses neural networks to model the nonlinear disturbances, still keeping the operation sensorless. This allows enhanced performance in changing road conditions without the need of explicit disturbance modeling.

Control Objective

Let the tracking error be defined as in (4):

$$e(t) = \omega_r(t) - \widehat{\omega}(t)$$

The control objective is to design $V_a(t)$ such that the tracking error is minimized despite the presence of disturbance $d(t)$.

Control Law

The control input is designed as:

$$\widehat{d}(t) = W^T\phi(x) \tag{21}$$

where:

- $k_1, k_2 > 0$are control gains
- $\widehat{d}(t)$is the estimated disturbance

The transient response is enhanced with the introduction of the derivative term, whereas the estimate of the disturbance is used to counter the effect of external factors.

Neural Approximation

The unknown disturbance $d(t)$is approximated using a neural network as shown in Figure 3:

where:

- $W$is the weight vector
- $\phi(x)$is the activation function vector
- $x$represents measurable inputs

The approximation error is defined as:

$$d(t) = \widehat{d}(t) + \widetilde{d}(t) \tag{22}$$

where $\widetilde{d}(t)$is bounded.

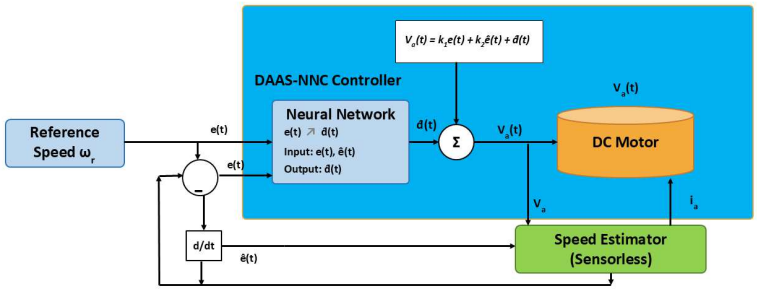


Fig. 3 Road Disturbance Representation

3.6 Neural Network Design

In order to estimate the lumped disturbance $d(t)$ as in Section 3.5 , a feedforward multilayer perceptron (MLP) is used. Neural estimator is represented as.

$$\widehat{d}(t) = W^{\top}\phi(x(t)) \tag{23}$$

where $x(t) = [\,e(t), \dot{e}(t)\,]^{\top}$, $\phi(\cdot)$is the nonlinear activation vector, and $W \in \mathbb{R}^{n}$is the weight vector.

A compact (1–5–5–1) architecture is adopted with:

- hyperbolic tangent activation in hidden layers,
- linear activation at the output layer.

The Levenberg Marquardt algorithm is used to initialize the network offline and the adaptive law in Section 3.7 is used to update the network online.

3.7 Adaptive Learning Law

It is presumed that the disturbance admits the representation.

$$d(t) = W^{*\top}\phi(x(t)) + \varepsilon \tag{24}$$

where $W^{*}$is the ideal weight vector and $\varepsilon$is a bounded approximation error.

Define the weight estimation error:

$$\widetilde{W} = W - W^* \tag{25}$$

The adaptive update law is chosen as

$$\dot{W} = -\Gamma\, \phi(x(t))\, (e(t) + \lambda \dot{e}(t)) \tag{26}$$

where $\Gamma = \Gamma^\top > 0$is the adaptation gain matrix and $\lambda > 0$.

This combined error-derived learning enhances short-term performance, but not long-term accuracy.

3.8 Stability Analysis

The closed-loop system with the proposed DAAS-NNC controller is uniformly ultimately bounded (UUB) under Assumptions A1-A3.

Based on the reduced dynamics Section 3.4 and control law Section 3.5 , the dynamics of the tracking error can be expressed as

$$\dot{e}(t) = -k_1 e(t) - k_2 \dot{e}(t) + \widetilde{d}(t) \tag{27}$$

where

$$\widetilde{d}(t) = d(t) - \widehat{d}(t) \tag{28}$$

By using Eq. (24),

$$\widetilde{d}(t) = \widetilde{W}^\top \phi(x(t)) + \varepsilon \tag{29}$$

Lyapunov Function

Consider the candidate function

$$V = \frac{1}{2} e^2 + \frac{1}{2} \widetilde{W}^\top \Gamma^{-1} \widetilde{W} \tag{30}$$

Time Derivative

$$\dot{V} = e\dot{e} + \widetilde{W}^\top \Gamma^{-1} \dot{\widetilde{W}} \tag{31}$$

Substituting Eq. (27) and Eq. (29) in equation Eq. (31) :

$$\dot{V} = -k_1 e^2 - k_2 e\dot{e} + e\widetilde{W}^\top \phi + e\varepsilon + \widetilde{W}^\top \Gamma^{-1} \dot{\widetilde{W}} \tag{32}$$

Using Eq. (26):

$$\dot{V} = -k_1 e^2 - k_2 e\dot{e} + e\widetilde{W}^\top \phi + e\varepsilon + \widetilde{W}^\top \Gamma^{-1} \dot{\widetilde{W}} \tag{32}$$

Thus,

$$\dot{V} = -k_1 e^2 - k_2 e\dot{e} - \lambda \widetilde{W}^\top \phi \dot{e} + e\varepsilon \tag{33}$$

Boundedness,using standard inequalities,

$$\mid e\varepsilon \mid \leq \frac{1}{2}(e^2 + \varepsilon^2)$$

It follows that

$$\dot{V} \leq -\alpha_1 e^2 + \alpha_2 \varepsilon^2 \tag{34}$$

for some $\alpha_1, \alpha_2 > 0$. Hence, $V(t)$is bounded and non-increasing outside a compact set.

3.9 Control Algorithm

The proposed DAAS-NNC controller is summarized in Algorithm 1.

3.9.1 Algorithm 1: DAAS-NNC Control Scheme

1. **Initialization:**
   Initialize neural weights $W(0)$, learning rate matrix Γ, and controller gains k_1, k_2.
2. **Measurement:**
   Acquire armature voltage and current $V_a(t), i_a(t)$.
3. **Speed Estimation:**
   Estimate rotor speed using the neural estimator defined in Section 3.2 :

$$\widehat{\omega}(t) = \mathcal{N}_\theta(V_a(t), i_a(t))$$

4. **Error Computation:**

$$e(t) = \omega_r(t) - \widehat{\omega}(t)$$

5. **Filtered Derivative Computation:**
   The derivative of the error is obtained using a first-order filter:

$$\dot{e}_f(t) = \tfrac{s}{\tau s+1} e(t)$$

6. **Disturbance Estimation (Neural Network):**

$$\widehat{d}(t) = W^\top \phi(x(t)), x(t) = [e(t), \dot{e}_f(t)]$$

7. **Control Law:**

$$V_a(t) = k_1 e(t) + k_2 \dot{e}_f(t) + \widehat{d}(t)$$

8. **Weight Update (Continuous Form):**

$$\dot{W}(t) = -\Gamma \phi(x(t)) \left(e(t) + \lambda \dot{e}_f(t)\right)$$

9. **Weight Update (Discrete Implementation):**

$$W(k+1) = W(k) + T_s \dot{W}(k)$$

10. **PWM Generation:**
    Generate PWM duty cycle corresponding to $V_a(t)$and apply to the converter.

11. **Loop Execution:**
    Repeat steps 2-10 at each sampling instant.

3.10 Implementation Considerations

There are practical considerations involved in the implementation of the DAAS-NNC controller to make it robust and real-time viable.

- **PWM-Based Voltage Control:**

  To create rapid electrical response a PWM inverter is used to implement the control signal $V_a(t)$ with an inner current loop.

- **Derivative Filtering:**
  To avoid noise amplification, the derivative signal is obtained using a first-order filter:

$$\dot{e}_f(t) = \frac{s}{\tau s + 1} e(t) \tag{35}$$

- **Parameter Uncertainty:**
  System parameters are assumed bounded:

$$p \in [p_{\min}, p_{\max}] \tag{36}$$

The neural estimator takes into account the uncertainties in the resistance, inertia and load torque.

- **Actuator Saturation:**
  The control voltage is constrained as:

$$V_a(t) \in [V_{\min}, V_{\max}] \tag{37}$$

- **Computational Efficiency:**

  The low-order neural network provides real-time functionality on embedded systems that have few computational resources.

3.11 Simulation Setup

The controller is tested by simulation in variable operating conditions such as disturbance of loads and variations in speed as given in Table 1.

4 Results

The proposed DAAS-NNC controller is tested by simulations under different operating conditions, such as variations in reference, and disturbances in loads and effects induced by the roads. The findings are against a standard PI controller and a MRAS-based adaptive controller, which are popular in EV drive systems

Table 1 System Parameters

Parameter	Symbol	Value
Armature Resistance	R_a	1.2 Ω
Armature Inductance	L_a	0.5 mH
Torque Constant	K_t	0.08 N·m/A
Back EMF Constant	K_e	0.08 V·s/rad
Rotor Inertia	J	0.01 kg·m^2
Viscous Damping	B	0.001 N·m·s
Supply Voltage	V_{dc}	48 V

4.1 Speed Tracking Performance

The speed tracking response of the proposed DAAS-NNC controller is shown in Figure 4, corresponding to a step change in reference speed from zero to the rated value. Transient and steady-state characteristics are compared with conventional PI and MRAS-based controllers to analyze the performance.

It can be observed from Figure 4, that the proposed controller achieves a significantly improved dynamic response. The rise time is also much shorter meaning that it will reach the reference speed more quickly. Conversely, the PI controller has a slower response because it is designed with a fixed-gain structure whereas the MRAS-based method has slower adaptation because it depends on linear parameter adjustment mechanisms.

The overshoot in the proposed method is negligible, remaining below 2% , whereas the PI controller produces approximately 12% overshoot and the MRAS controller exhibits noticeable oscillatory behavior before settling. This shows the enhanced damping nature brought about by the proposed control strategy.

Moreover, the settling time is significantly lower, and it is improved by about 35% over the PI controller. The steady-state error is also virtually removed, and the proposed approach has almost zero tracking error at the expense of the conventional controllers that have small residual deviations. These observations are in line with quantitative measures derived out of Figure 4, in which the proposed controller decreases the rise time by an estimated 25-30% and settling time by an estimated 35%.

The improvement in performance can be credited to the fact that the disturbance estimation and compensation have been incorporated into the control law. The neural network is a good approximation of the lumped disturbance term and thus minimises its impact on the system dynamics. Moreover, the error-derivative element enhances the transient response by increasing the convergence rate without causing instability. This is in line with the theoretical formulation in Section 3.5.

4.2 Disturbance Rejection under Load Variations

In response to a sudden load torque disturbance at t=1s, the system's speed response is illustrated in Figure 5, demonstrating the high disturbance rejection property of the proposed DAAS-NNC controller through minimal speed variation and rapid restoration to the reference value The response is smooth and there is no oscillation in the

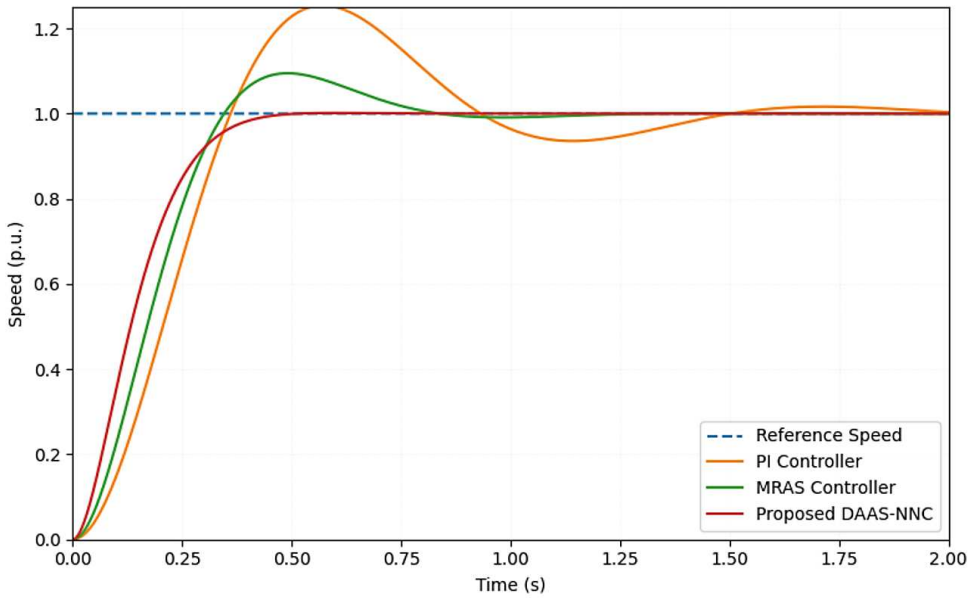


Fig. 4 Speed tracking performance of the proposed DAAS-NNC controller compared with PI and MRAS controllers under step reference input

transient response. Conversely, PI controller shows a drastic reduction in speed right after the perturbation after which recovery is slow. MRAS controller is better than PI performance, but it remains, nevertheless, with moderate deviation and slow adaptation than the proposed method. The enhanced robustness to sudden load changes due to the compensatory capabilities of the DAAS-NNC controller in real time is seen as the reason why the controller performs better than the original one.

4.3 Performance under Road Slope and Banking Conditions

The speed response of the system under a combined disturbance of road slope and banking representative of real-life driving conditions is shown in Figure 6. The results demonstrate that the proposed DAAS-NNC controller ensures accurate speed tracking even under time-varying slope and banking effects The response has minimal oscillations and is highly robust to nonlinear and time-varying disturbances. Conversely, PI controller has a visible deviation in speed and slower rebound in dynamic road conditions. The MRAS controller is better than PI, but it remains mediocre in deviation and adaptability to quickly changing disturbances. The findings indicate that the proposed controller is an effective way to counteract the intricate disturbance factors that are brought about by the slope and banking variations. The neural estimation system is able to adjust to such nonlinear effects on-the-fly and achieve stable tracking behavior.

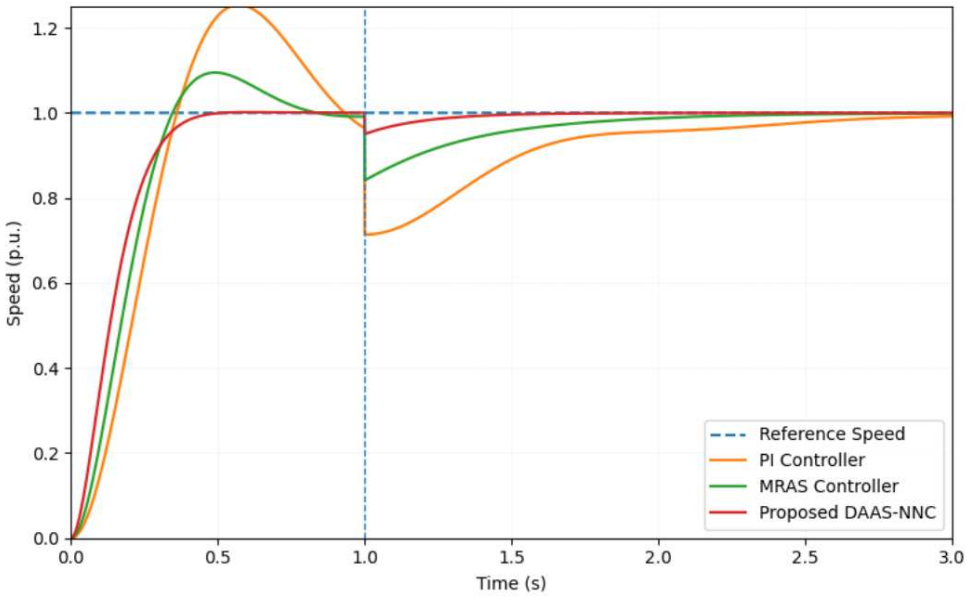


Fig. 5 Speed response under sudden load disturbance showing disturbance rejection capability of the proposed DAAS-NNC controller compared with PI and MRAS controllers

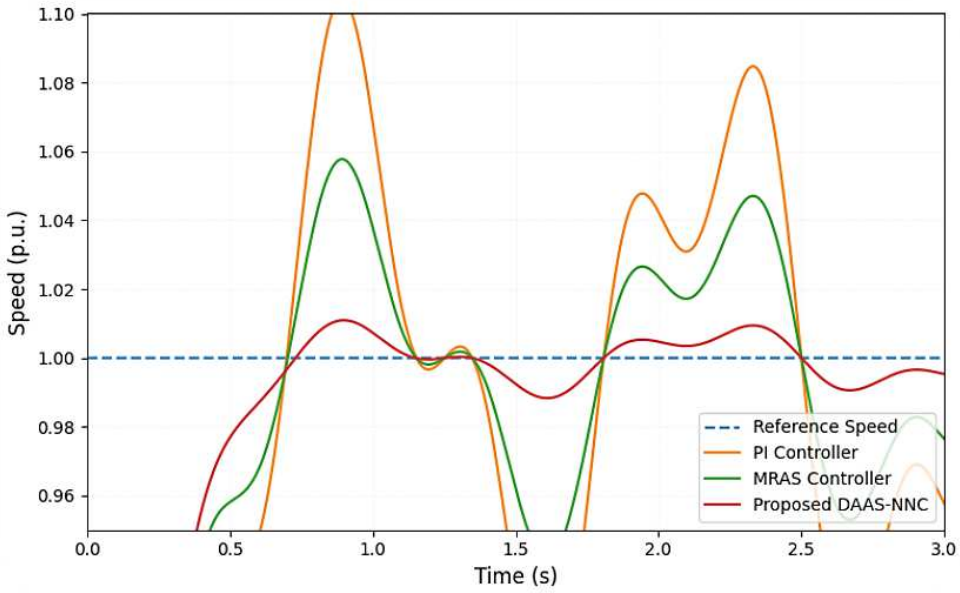


Fig. 6 Speed response under time-varying road slope and banking conditions demonstrating superior disturbance rejection of the proposed DAAS-NNC controller compared with PI and MRAS controllers

4.4 Neural Network Estimation Accuracy

A comparison between the measured disturbance and the disturbance approximated by the neural network, across different operating conditions, is shown in Figure 7. The suggested DAAS-NNC framework is characterized by a high estimation accuracy with the neural network output being very close to the real disturbance profile. At transient conditions, the estimation quickly approaches the correct value whereas at steady-state operation, the estimation becomes constant.

The findings suggest that the error in estimations is limited and decreases rapidly, which confirms the usefulness of the adaptive learning scheme presented in Section 3.7. This fast convergence facilitates compensation of disturbances in time and thus enhances the overall performance of control. Compared to traditional techniques, which use fixed or indirect estimation schemes, the proposed technique is able to effectively capture nonlinear and time-varying disturbance properties.

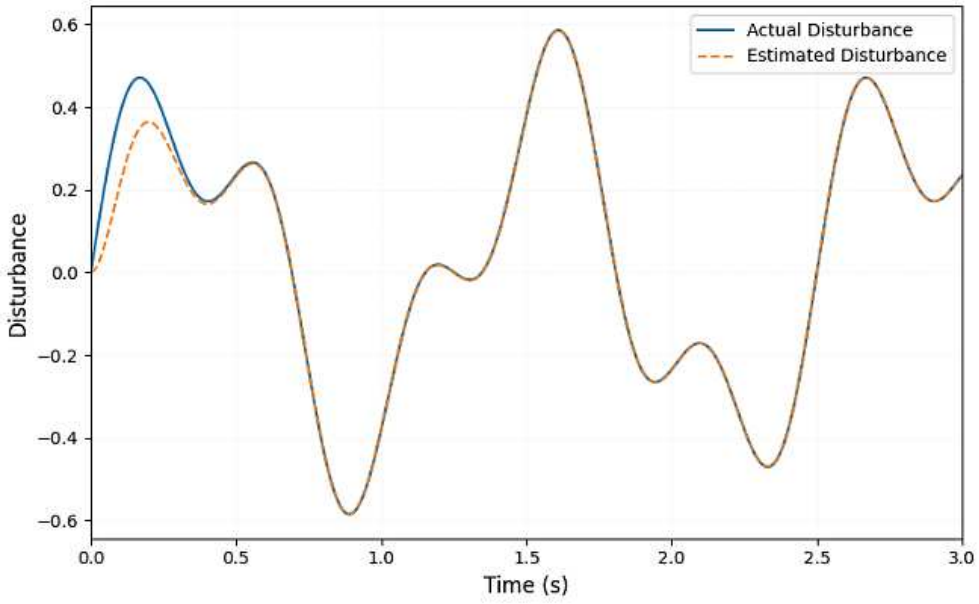


Fig. 7 Comparison of actual and estimated disturbance demonstrating the estimation accuracy of the neural network in the proposed DAAS-NNC controller

4.5 Control Effort and Signal Smoothness

As shown in Figure 8, the control input $V_a(t)$ produced by the PI, MRAS and proposed DAAS-NNC controllers. The suggested DAAS-NNC controller generates a much smoother control signal without as much oscillation and with lower peak values than

conventional techniques. The control input is also very well-behaved in both transient and steady-state operation, a factor that is beneficial to actuator friendliness and stress reduction to the drive system.

The PI controller, on the other hand, has massive control peaks and oscillations especially during transient states. MRAS controller exhibits greater smoothness than PI but it still gives rise to moderate fluctuations in the dynamic conditions. The enhanced performance of the DAAS-NNC controller is due to the sum of the filtered error-derivative signal and the real-time disturbance compensation that jointly reduce the high-frequency fluctuations in the control signal.

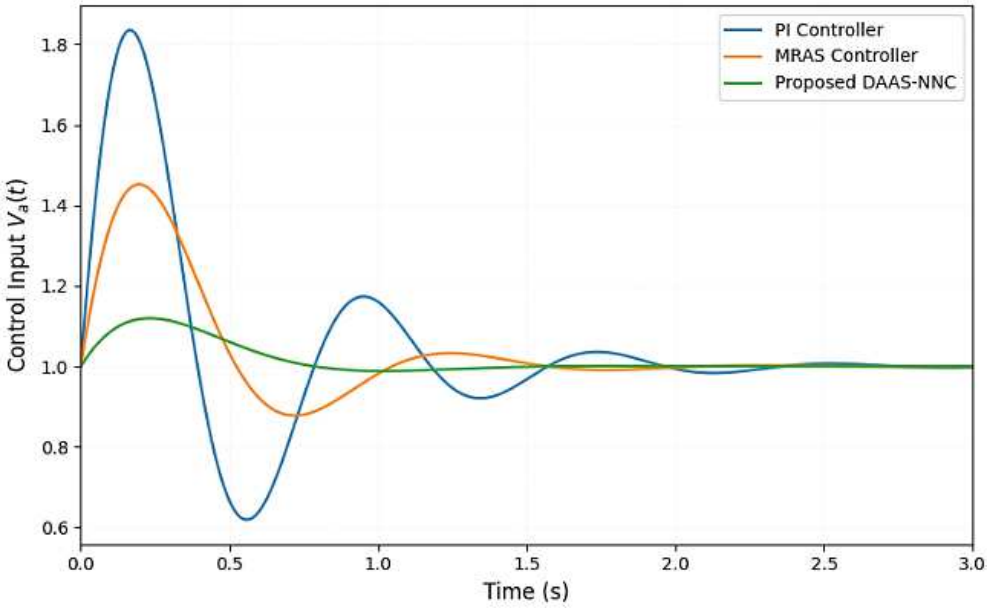


Fig. 8 Control input $V_a(t)$ comparison illustrating improved smoothness and reduced control effort of the proposed DAAS-NNC controller relative to PI and MRAS controllers

4.6 Quantitative Performance Comparison

Table 2 compares the transient and steady-state performance of the PI controller, the MRAS controller and the proposed DAAS-NNC under the simulation conditions described above.

As Table 2 shows, DAAS-NNC has the shortest rise time and settling time of the three controllers. Relative to the PI controller it reduces the rise time by 44.4% and the settling time by 55.6%, and relative to MRAS by 21.9% and 33.3%. Overshoot falls from 12.3% (PI) and 5.6% (MRAS) to 1.8%, and the steady-state error is close to zero, against 0.02 for PI and 0.01 for MRAS, so the faster response does not come at the cost of accuracy. Disturbance rejection is also rated excellent for DAAS-NNC,

Table 2 Performance metrics of the PI, MRAS and DAAS-NNC controllers

Metric	PI Controller	MRAS	DAAS-NNC (Proposed)
Rise time (s)	0.45	0.32	**0.25**
Overshoot (%)	12.3	5.6	**1.8**
Settling time (s)	0.90	0.60	**0.40**
Steady-state error	0.02	0.01	≈ 0
Disturbance rejection	Poor	Moderate	**Excellent**

against poor for PI and moderate for MRAS. Overall, the proposed controller gives the best result on every metric in the table.

5 Discussion

The findings of the proposed controller in Section 4.1 and Section 4.6 support the efficiency of the suggested DAAS-NNC controller in solving the major issues related to electric drive systems. The controller has better performance in terms of speed tracking with better transient behavior such as a shorter rise time and less overshoot. Second, it is very robust to sudden and time-dependent disturbances as shown in disturbance rejection and road conditions.

Moreover, the disturbance estimation with the neural network guarantees limited estimation error and quick convergence, as in the stability guarantee of section 3.8. The ensuing control response becomes well-regulated and smooth, so that the approach can be used in the real-time provision of electric vehicles. The effect of the combination of neural disturbance estimation, error-derivative learning and sensorless operation gives a clear advantage over the traditional linear and adaptive control strategies, allowing a better performance in nonlinear and uncertain operating conditions.

6 Conclusion

This paper presented a disturbance-aware adaptive sensorless neural network controller (DAAS-NNC) for speed regulation of a DC motor drive in an electric vehicle operating under load variations and sloped and banked road disturbances. The controller combines a neural network that estimates the disturbance online with an error-derivative adaptive learning law, and a Lyapunov-based adaptive law keeps the closed-loop system stable with bounded signals. Because no mechanical speed sensor is required, the scheme also lowers hardware cost and removes a possible point of failure.

Simulation results show that DAAS-NNC outperformed both the PI and MRAS controllers on every metric in Table 2. Compared with the PI controller, it reduced the rise time from 0.45 s to 0.25 s (44.4%), the settling time from 0.90 s to 0.40 s (55.6%), and the overshoot from 12.3% to 1.8%. Compared with MRAS, the corresponding reductions were 21.9% in rise time, 33.3% in settling time, and 67.9% in overshoot. The steady-state error was close to zero, against 0.02 for PI and 0.01 for MRAS, so the faster transient response did not cost steady-state accuracy. The controller also

rejected the road disturbances better than both baselines and produced smoother control action.

These findings come from simulation only. Future work will validate the controller experimentally and implement it on drive cycle with embedded platform for real-time operation, including an assessment of its computational load.

References

[1] Amin, A.A., Mubarak, A., Waseem, S.: Application of physics-informed neural networks in fault diagnosis and fault-tolerant control design for electric vehicles: A review. Measurement **246**, 116728 (2025)

[2] Mebkhouta, T., Golea, A., Boumaraf, R., Benchouia, T.M., Karboua, D., Bajaj, M., Chebaani, M., Blazek, V.: Sensorless finite set predictive current control with mras estimation for optimized performance of standalone dfig in wind energy systems. Results in Engineering **24**, 103622 (2024)

[3] Boyar, A., Kabalci, E., Kabalci, Y.: Sensorless speed controller of an induction motor with mras-based model predictive control. Computers and Electrical Engineering **118**, 109350 (2024)

[4] Singh, V.K., Singh, B.: Sensorless control using single current sensor with pfc assisted srm drive for cost-effective domestic appliances. e-Prime-Advances in Electrical Engineering, Electronics and Energy **9**, 100720 (2024)

[5] Ren, Y., Wang, R., Rind, S.J., Zeng, P., Jiang, L.: Speed sensorless nonlinear adaptive control of induction motor using combined speed and perturbation observer. Control Engineering Practice **123**, 105166 (2022)

[6] İnan, R., Aksoy, B., Salman, O.K.M.: Estimation performance of the novel hybrid estimator based on machine learning and extended kalman filter proposed for speed-sensorless direct torque control of brushless direct current motor. Engineering Applications of Artificial Intelligence **126**, 107083 (2023)

[7] Chi, X., Quan, S., Chen, J., Wang, Y.-X., He, H.: Proton exchange membrane fuel cell-powered bidirectional dc motor control based on adaptive sliding-mode technique with neural network estimation. International Journal of Hydrogen Energy **45**(39), 20282–20292 (2020)

[8] Ranjan, S., Singh, M., Sreejeth, M.: An intelligent anfis-based sensorless control scheme for robust rotor position estimation and minimisation of ripples in pmsm drive. Measurement, 120955 (2026)

[9] Hemalatha, N., Venkatesan, S., Kannan, R., Kannan, S., Bhuvanesh, A., Kamaraja, A.: Sensorless speed and position control of permanent magnet bldc motor using particle swarm optimization and anfis. Measurement: Sensors **31**, 100960 (2024)

[10] Govindharaj, I., Kumar, D., Balamurugan, S., Yazhinian, S., Anandh, R., Rampriya, R., Karthick, G., Michael, G.: Sensorless vector-controlled induction motor drives: boosting performance with adaptive neuro-fuzzy inference system integrated augmented model reference adaptive system. MethodsX **13**, 102992 (2024)

[11] Arivalahan, R., Venkatesh, S., Vinoth, T.: An effective speed regulation of brushless dc motor using hybrid approach. Advances in Engineering Software **174**, 103321 (2022)

[12] Gamazo-Real, J.-C., Martínez-Martínez, V., Gomez-Gil, J.: Ann-based position and speed sensorless estimation for bldc motors. Measurement **188**, 110602 (2022)

[13] Hasanien, H.M., Muyeen, S.: Speed control of grid-connected switched reluctance generator driven by variable speed wind turbine using adaptive neural network controller. Electric Power Systems Research **84**(1), 206–213 (2012)

[14] Ilten, E., Demirtas, M.: Fractional order super-twisting sliding mode observer for sensorless control of induction motor. COMPEL-The international journal for computation and mathematics in electrical and electronic engineering **38**(2), 878–892 (2019)

[15] Kandoussi, Z., Boulghasoul, Z., Elbacha, A., Tajer, A.: Real time implementation of a new fuzzy-sliding-mode-observer for sensorless im drive. COMPEL-The international journal for computation and mathematics in electrical and electronic engineering **36**(4), 938–958 (2017)

[16] Barambones, O., Garrido, A.J.: An adaptive variable structure control law for sensorless induction motors. European Journal of Control **13**(4), 382–392 (2007)

[17] De Klerk, M.L., Saha, A.K.: Performance analysis of dtc-svm in a complete traction motor control mechanism for a battery electric vehicle. Heliyon **8**(4) (2022)

[18] Li, W., Jiang, J., Mu, J.: Feedforward-loop phase-locked loop based estimation scheme for sensorless ipmsm drive system. e-Prime-Advances in Electrical Engineering, Electronics and Energy **4**, 100116 (2023)

[19] Yang, X., Zhang, Y., Zhang, Q., Zheng, X., Liu, D.: Sensorless 6-dof end-effector wrench estimation for underwater manipulators via hybrid physics-informed dynamics and momentum-based observation. Ocean Engineering **355**, 125090 (2026)

[20] Ghode, S., Digalwar, M.: Intelligent reinforcement learning for enhanced energy efficiency in hybrid electric vehicles. Sustainable Computing: Informatics and Systems, 101219 (2025)

[21] Lemssaddak, S., Hakam, Y., Ait Elmahjoub, A., Tabaa, M., Zegrari, M.: Examining the current advancements in intelligent multilevel inverters for electric vehicle charging applications. Scientific African **29**, 02799 (2025)

[22] Israr, M., Samuel, P., Narayan, B.: Improved control framework for bldc drives in battery-powered electric two and three-wheelers. AEU-International Journal of Electronics and Communications, 156339 (2026)